Supporting Information (Supplemental Material and Methods, 5 Supplemental Figures, 14 Supplemental Tables, and Supplemental References)

Supplemental Material and Methods

Alzheimer's Disease Neuroimaging Initiative (ADNI) cohort

We obtained genotype, transcriptome, and biomarker data from the Alzheimer's Disease Neuroimaging Initiative (ADNI) database (adni.loni.usc.edu). The ADNI was launched in 2003 as a public–private partnership and is led by Principal Investigator Michael W. Weiner, MD. The primary goal of the ADNI is to test whether serial MRI, PET, other biological markers, and clinical and neuropsychological assessments can be combined to measure the progression of MCI and AD. Array genotyping data from the ADNI-1 (n = 757) and ADNI-GO/2 (n = 432) generated from the HumanOmniExpress BeadChip (Illumina) were adopted for our replication studies, with another dataset derived from whole-genome sequencing of ADNI subjects (n = 808; among whom, 258 overlapped with subjects from ADNI-1, 427 overlapped with ADNI-GO/2, and 123 were newly recruited subjects). We determined the phenotypes for the ADNI subjects on the basis of the latest diagnostic records (updated until July 2016). By combining the subjects from the three datasets, we obtained genotype information for 1,312 subjects (n = 1,312) including 515 AD and 339 NC subjects (Remaining subjects were in MCI status).). For blood transcriptome data, please refer to (1) for details. For cerebrospinal fluid (CSF) and plasma biomarker levels, data were obtained from the Biomarkers Consortium Projects entitled "Use of Targeted Multiplex Proteomic Strategies to Identify Novel CSF Biomarkers in AD" and "Use of Targeted Multiplex Proteomic Strategies to Identify Plasma-Based Biomarkers in Alzheimer's Disease" accordingly. Please refer to the corresponding project descriptions for details. (https://adni.loni.usc.edu/wp-content/uploads/2010/11/BC_Plasma_Proteomics_Data_Primer.pdf; https://fnih.org/what-we-do/biomarkers-consortium/programs/alzheimers-targeted-csf-based-proteomics).

NIA Alzheimer's Disease Centers Cohort (ADC)

Genotype and phenotype data were retrieved from the NIH dbGaP (accession number: phs000372.v2.p1) for an AD cohort comprising 6,065 subjects (n = 6,065), with individual genotypes generated from a Human660W-Quad BeadChip (Illumina) or HumanOmniExpress Array (Illumina). All autopsied subjects were ≥60 years old at death. Dementia in AD cases was determined according to the DSM-IV criteria or a Clinical Dementia Rating (CDR) ≥1.

Please refer to the corresponding dbGaP project for details (2, 3). We only kept subjects with a definite diagnosis of AD as well as NCs, finally yielding 5,692 subjects (AD: 3,946, NC: 1,746) for the replication study.

Late Onset Alzheimer's Disease (LOAD) Family Study

Genotype and phenotype data were retrieved from the NIH dbGaP (accession number: phs000168.v2.p2), which included four datasets. The genotype information of 5,192 subjects (n = 5,192) from sets No. 1, 3, and 4 (General Research Use, disease-specific [Alzheimer's disease] and disease-specific [Alzheimer's disease, NPU], respectively) were merged before the subsequent analysis. Individual genotypes were generated from a 610K Beadchip array (Illumina). Please refer to the corresponding dbGaP project for details (4). We only kept NCs or subjects with a definite diagnosis of AD, finally yielding 2,695 subjects (AD: 464, NC: 2,231) for the replication study.

Filtering and imputation for the array dataset

We converted the array genotype information (ADNI, LOAD, and ADC) from PLINK file format (5) to VCF file format using VcfCooker (v1.1.1) (https://genome.sph.umich.edu/wiki/VcfCooker) and performed pre-filtering with a sample call rate ≥ 95% and an SNP call rate ≥ 80% for each genotype file. The filtered genotype information was submitted to the Michigan Imputation Server using EAGEL (v2.3) with Haplotype Reference Panel (HRC r1.1) for phasing and imputation (6-8) in the form of chromosome-separated VCF files. Post-filtering was further applied by filtering imputed variants with imputation R^2-values < 0.3.

Whole-genome sequencing

For WGS, we collected whole blood in non-EDTA tubes and centrifuged them at 2000 × g. After removing the serum in the supernatant, we used the cell pellet to prepare genomic DNA. genomic DNA purity was checked by a NanoPhotometer® spectrophotometer (Implen), the concentration was measured using a Qubit® DNA Assay Kit with a Qubit® 2.0 Fluorometer (Thermo Fisher Scientific), and fragment size distribution was measured using the DNA Nano 6000 Assay Kit with the Bioanalyzer 2100 system (Agilent). DNA (1.5 μg) of each sample was

fragmented by sonication to 350 bp and used to generate a sequencing library with the Truseq Nano DNA HT Sample Preparation Kit (Illumina). The genomic DNA libraries were sequenced. To ensure data quality, adapter contamination and low-quality reads were filtered from the raw data, producing clean data with a base quality greater than Q20 for most detected signals; the proportion of Q30 exceeded 80%.

Microarray-based genotyping

For QC analysis, we used microarray-based genotyping as an independent assay to verify the SNP call results from low-coverage WGS. We genotyped genomic DNA from 96 out of 1,222 subjects (~8%) using the Axiom® Genome-Wide CHB 1 & CHB 2 Array Plate Set (Affymetrix), which was specifically designed for the Chinese population. Genotyping was performed on an Illumina array platform (Beijing Genomics Institute). We filtered the results according to an SNP call rate ≥ 95% and retained 937,176 concordantly detected bi-allelic variants with a minor allele frequency (MAF) ≥ 5% in the WGS dataset for the quality control assessment.

Whole genome sequencing (WGS) and variant calling method

For variant detection, the Gotcloud (9) pipeline was adopted to detect variants from our low-pass WGS data comprising 1,348 samples including 126 re-sequenced samples. Data were subsequently subjected to *FastQC* (v0.11.2) (10) for quality checking and *Trimmomatic* (v 0.32) (11) for the trimming and filtering of low-quality reads (*LEADING:3 TRAILING:3 SLIDINGWINDOW:4:15 MINLEN:40 ILLUMINACLIP: 2:30:10*). Clean data were mapped to the GRCh37 reference genome containing the decoy fragments (hs37d5.fa) using *BWA –mem* (v 0.7.12-r1039). After de-duplication and clipping of the overlapped pair-end reads, BAM files were subjected to samtools-hybrid (v0.1.7-hybrid [r510 + r983]), a specialized version of *samtools*, to generate glf files, which store the marginal likelihoods for genotypes (*-q 20 -F 0x0704* for filtering of low mapping quality and PCR duplication). glfFlex was adopted for the population-based SNP calling *(-p 0.9 --minMapQuality 0 --maxDepth 100000 --uniformTsTv, --smartFilter*), with a total of 24,742,555 single nucleotide variants obtained after variant calling. We applied hard-filtering methods implemented in the Gotcloud pipeline as VcfCooker (v1.1.1) to filter low-confidant variant calls on the basis of multiple metrics such as distance with known insertion/deletion sites (*--winIndel 5* using insertion deletion information obtained

from Mills and 1000G gold standard indels file), allele balance (*--maxABL 70*), and mapping quality (*--minMQ 20 --minQual 5*). We subjected variants with high-confidence calls in the range of minor allele frequency (MAF) ≥ 5% (*n* = 5,523,365; 22.3% of raw detected sites, 5,369,369 of which were in autosomal chromosomes) to Beagle (r1399) (12, 13) for phasing (*phase-its = 30*) and imputation (*impute-its = 15*) using the genotype likelihood information in chromosome-separated VCF files (*gl* flag).

Quality control assessment of variant detection

To assess the accuracy of variant detection, we re-sequenced 126 out of 1,222 samples (10.3% of all samples) using the same WGS protocol, together with 96 samples (7.9% of total samples) genotyped using the Axiom® Genome-Wide CHB 1 & CHB 2 Array Plate Set (Affymetrix). We obtained genomic DNA for quality control assessment from separate aliquots. We merged the re-sequenced samples into the whole cohort for SNP detection, phasing, and imputation. We used VCFtools (v0.1.14) (14) together with R programing to extract site information and subgrouped the autosomal variants according to average sequencing coverage (DP) and MAF. We stored genotype information in VCF format and subjected the information to *GATK GenotypeConcordance* (v3.4-46-gbc02625) to compare genotypes from two datasets. We calculated metrics for quality assessment including non-reference sensitivity (NRS), non-reference discrepancy (NRD), and overall concordance rate (CR) as follows:

$$NRS = \frac{\#\ true\ positive}{\#\ true\ polymorphic}$$

$$NRD = 1 - \frac{\#\ HOM\_VAR\_HOM\_VAR\ +\ \#\ HET\_HET}{total\ excluding\ \#\ HOM\_REF\_HOM\_REF}$$

$$CR = \frac{\#\ concordant\ genotypes}{\#\ genotypes}$$

We excluded the samples with re-sequenced discordant rate >5%. We performed sample quality control for gender consistency, and excluded related samples, removed population outlier using principal component analysis and confirmed our population structure using 1000 Genomes data. We filtered out the SNPs that failed in Hardy–Weinberg equilibrium

(HWE) in controls ($p < 1 \times 10^{-5}$).

Gender missingness or inconsistency

We converted phased and imputed genotype information from the WGS data of 1,222 samples into PLINK binary pedigree format and subjected it to PLINK (v1.9) *--check-sex* to estimate gender using genetic information from common variants in the X chromosome on the basis of calculated inbreeding coefficients (n = 153,276 for variants in the X chromosome). We excluded 16 samples (NC: 8, MCI: 5, AD: 2) from the data owing to a lack of gender information or inconsistency between sequencing data and clinical records.

Principal component analysis for outlier removal and correction of population structure

We subjected the remaining 1,206 samples to EIGENSOFT (v7.2.1) *smartpca* (15, 16) for principal component analysis to evaluate possible stratification rendered by admixed populations or batch effects during sequencing. We subjected genotype information from pruned autosomal SNPs (using PLINK *--indep-pairwise 50 5 0.2*, yielding 319,892 generated sites) to *smartpca* with a cutoff of six standard deviations and 10 iterations of outlier removal. As a result, we excluded 32 samples (NC: 22, MCI: 2, AD: 8) owing to deviation from main populations. We also used EIGENSOFT *smartpca* to generate principal components to correct for possible confounding factors in the combined dataset (i.e., the in-house cohort and the CONVERGE population control) during the association test.

Sample relatedness

We further subjected the remaining 1,174 samples to PLINK to examine sample relativeness using the pairwise identity-by-state (IBS) distance generated by PLINK *--matrix.* We set an IBS distance (IBD) > 0.1875 as a threshold, which is halfway between the expected IBD for third- and second-degree relatives. We excluded two samples (AD: 1, NC: 1) from the data and kept the remaining 1,172 samples (NC: 442, MCI: 253, AD: 477) for the association analysis.

Population structure and estimation of ethnic attributes

We subjected the genotype information obtained from 168,673 pruned concordant calls

with an MAF ≥ 10% in 1,172 Chinese AD WGS subjects together with 2,504 1000 Genomes Phase 3 data including five super-populations (African [AFR], *n* = 661; European [EUR], *n* = 503; East Asian [EAS], *n* = 504; South Asian [SAS], *n* = 489; American [AMR], *n* = 347) to *fastStructure* (17) (*K* = 5) to infer the ethnic attributes of our in-house data. Meanwhile, we subjected 5,181,985 concordant calls to PLINK --*pca* to visualize population structure and attributes in comparison with 1000 Genomes Phase 3 dataset.

Filtering of low-confidence SNP calls

During the association test using the PLINK, we controlled for Hardy–Weinberg equilibrium (HWE) by setting a *p*-value threshold of 1×10^{-5} for normal controls from the in-house WGS and CONVERGE datasets. After obtaining the association results, we assessed the sites with a discordant call rate > 5% (5 of 126 samples) among 126 re-sequenced samples and filtered them (516,773 sites, 9.62% of autosomal sites with an MAF ≥ 5%) to overcome the possible issues in detection of variants in low-complexity or repetitive regions.

TaqMan genotyping for *APOE*

For *APOE*-ε4 (rs429358 and rs7412), we performed genotyping by using the TaqMan assay with probe ordered from Thermo Scientific (assay ID: C_3084793_20 and C_904973_10). We subjected 10 ng genomic DNA to real-time PCR on the QuantStudio 7 Flex Real-Time PCR system (Applied Biosystems) and performed genotype calling using QuanStudio Real-Time PCR software (Applied Biosystems). We used R programming for the statistical analysis of genotyping results.

Genotype expression analysis for candidate sites in transcriptome data

The Genotype-Tissue Expression (GTEx) Project was supported by the Common Fund of the Office of the Director of the National Institutes of Health, and by NCI, NHGRI, NHLBI, NIDA, NIMH, and NINDS (18, 19). The data used for the analyses described in this manuscript were obtained from dbGaP (phs000424.v6.p1). We imputed genotype data using the Michigan Imputation Server (EAGEL v2.3) with the Haplotype Reference Panel (HRC r1.1) (6-8). For network analysis, RNA-seq datasets from blood (*n* = 365) and hippocampal tissues (*n* = 87) were included, and low-abundance genes (average Reads Per Kilobase of transcript per Million

mapped reads [RPKM] < 1 in corresponding tissues) were filtered out prior to the analysis. For the global genotype–expression analysis, 52 variants (*GCH1*: 1, *KCNJ15*: 2, *APOE* locus: 49) that passed the nominal *p*-value threshold of 5E−08 during the stage 1+2 analysis and were concordantly detected in the imputed GTEx dataset were subjected to robust linear regression using R *robustbase* packages, further adjusting for the first three principal components, age, and gender. The expression levels (i.e., RPKM) for each gene across individuals with the same tissue samples were normalized by the rank-based inverse normal transformation (INT) method using the *rntransform* function in the R *GenABEL* package (20) to overcome the possible outliers. We filtered out gene-SNP association pairs with raw *p*-value > 0.05. Then, for each of the three loci, we obtained the top 100 genes (based on gene-level *p*-values, where a gene-level *p*-value is the smallest *p*-value from all SNPs tested in the locus) for network analysis. We finally reported the enriched gene ontology terms in the obtained network on the basis of a false-discovery rate (FDR) < 0.05. The regulatory network was visualized by using the R *ggnet2* package. For *GCH1*, RNA-seq data obtained from the brain caudate region (n = 94) was included for the genotype-expression association test using ANCOVA (analysis of covariance) model with age, gender and top-3 principal components.

Genotype-expression analysis of plasma and cerebrospinal fluid biomarker data for candidate sites

For plasma biomarkers retrieved from ADNI, markers with signals below the detection limit were filtered out before the association analysis. Genotype-expression analysis was first conducted by robust regression with the inclusion of age, gender and top-5 PCs as covariates to initial screen for possible hints in AD subjects. Biomarkers passed statistical significance threshold of $p = 0.05$ were recorded as potential candidates and ranked by *p*-value (from lowest to highest). For top-3 plasma biomarkers for KCNJ15 and GCH1, the biomarker levels (in log10 scale) were converted to the actual concentration values, with IQR filtering being applied to remove the outlier within individuals from same genotype and phenotype groups (values below Q1 − 1.5 × IQR or above Q3 + 1.5 × IQR were excluded) [Q1: first quartile; Q3: third quartile; IQR: inter-quartile range = Q3 − Q1]. Then clean data were subjected to ANCOVA model adjusting for age, gender and top-5 PCs with Bonferroni correction for further examination of possible regulation of biomarker levels between different phenotypes and

219 genotypes (within each genotypes the differences between AD and normal controls were tested;
220 within each phenotypes the differences in biomarkers level between genotypes were tested by
221 setting the homozygous reference groups as reference controls).
222

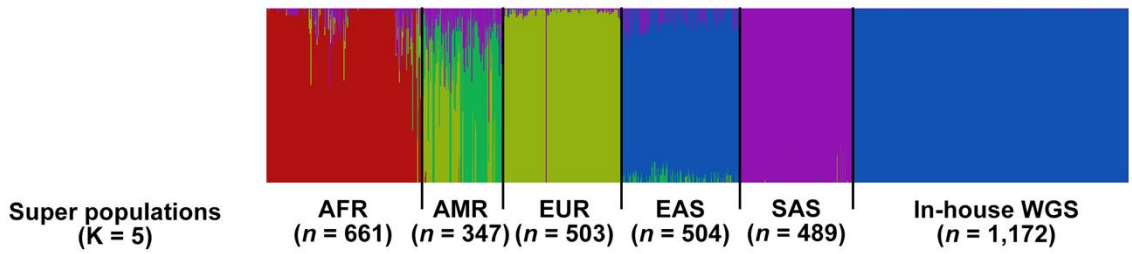

Figure S1. Mapping the ethnic attributes of the Chinese WGS cohort using the 1000 Genomes Super-population information. Genomic information from 2,504 1000 Genomes phase 3 individuals across 5 super-populations was used as a reference to infer the ethnic attributes of 1,172 in-house Chinese WGS samples. A total of 168,673 pruned ($R^2 < 0.2$) bi-allelic SNPs with an MAF ≥ 10% in in-house WGS data that were concordantly detected in the 1000 Genomes data were subjected to fastSTRUCTURE for clustering. Each subject is represented by a vertical line further partitioned into colored segments; lengths represent the admixture proportions from 5 clusters, with colors specifying the corresponding ethnic attributes. The results suggest that our in-house WGS data (dominantly shown in blue) fit into the EAS cluster (also dominantly shown in blue). AFR, African; AMR, American; EUR, European; EAS, East Asian; SAS, South Asian; MAF, minor allele frequency; SNP, single nucleotide polymorphism; WGS, whole-genome sequencing.

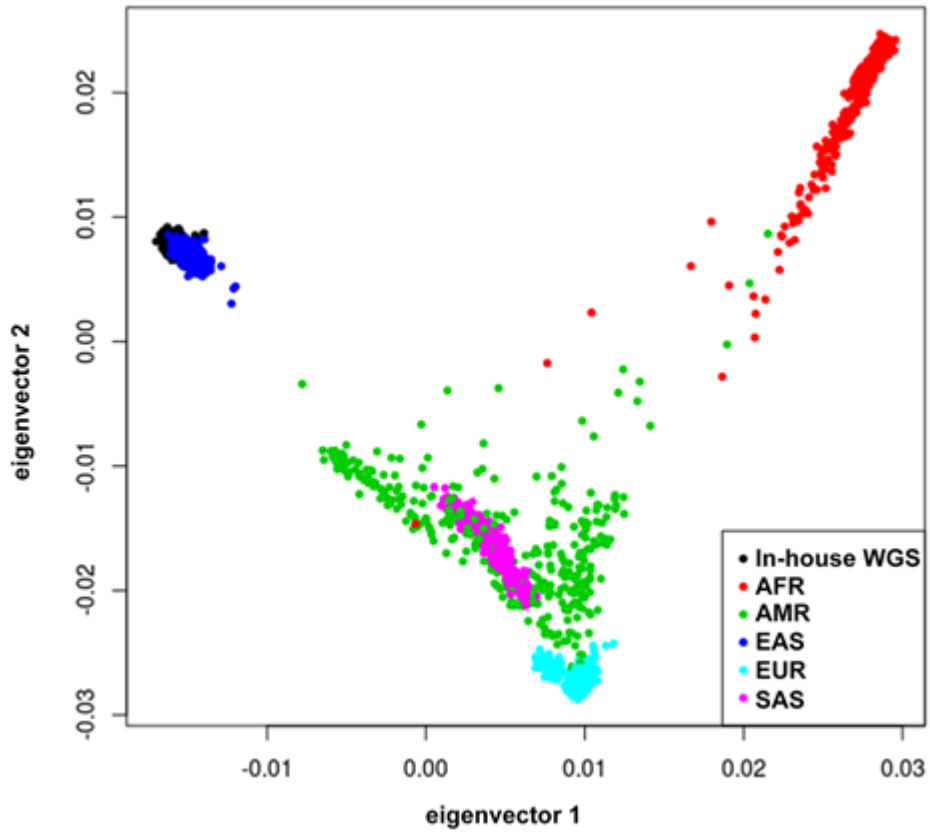

Figure S2. Mapping the ethnic attributes of the Chinese WGS cohort using the 1000 Genomes Super-population information: Principal component analysis (PCA). Genomic information from 2,504 1000 Genomes Phase 3 individuals across 5 super-populations was used as a reference to infer the ethnic attributes of 1,172 in-house WGS samples. A total of 5,181,985 bi-allelic SNPs with an MAF ≥ 5% in the WGS concordantly detected in the 1000 Genomes data were subjected to PCA. The X- and Y-axes denote PC1 and PC2 obtained from the PCA, respectively. Each dot in the figure represents one individual, and colors specify attributes. The plot suggests that our in-house WGS data (black) fit into the EAS supercluster (blue), as indicated by the overlap of these 2 populations. AFR, African; AMR, American; EUR, European; EAS, East Asian; SAS, South Asian; SNP, single nucleotide polymorphism; MAF, minor allele frequency; WGS, whole-genome sequencing; PCA, principal component analysis.

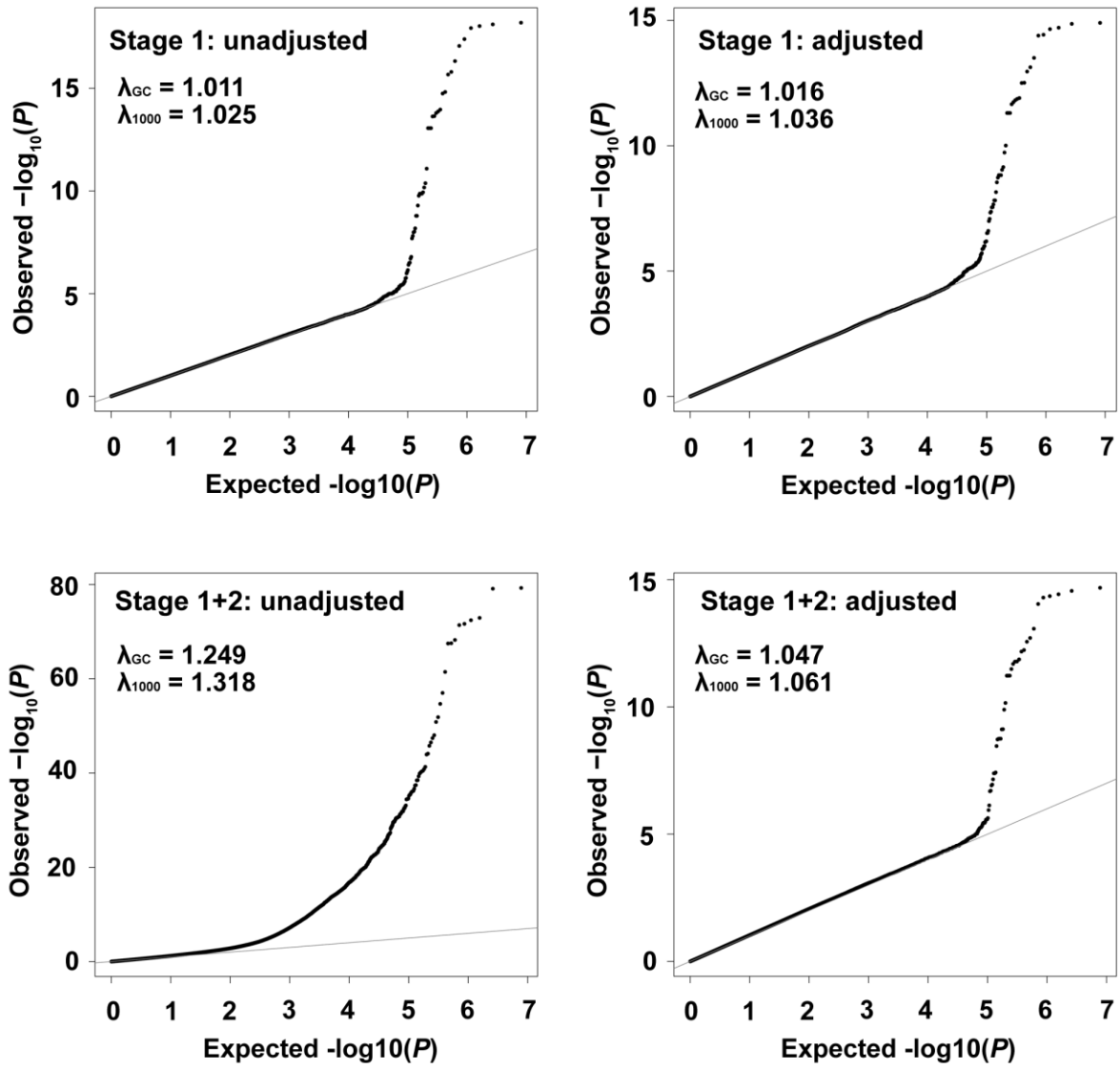

Figure S3. Quantile–quantile plot of the GWAS results of the WGS dataset. Quantile–quantile plot showing the *p*-value destitution for the stage 1 and stage 1+2 analyses before and after adjusting for age, gender, and phenotype-associated PCs. Values of genomic inflation factor (λ_{GC}) and factor for an equivalent study of 1000 cases and 1000 controls (λ_{1000}) are indicated (1.011 and 1.025 for λ_{GC} and λ_{1000}, respectively). GWAS, genome-wide association study; WGS, whole-genome sequencing.

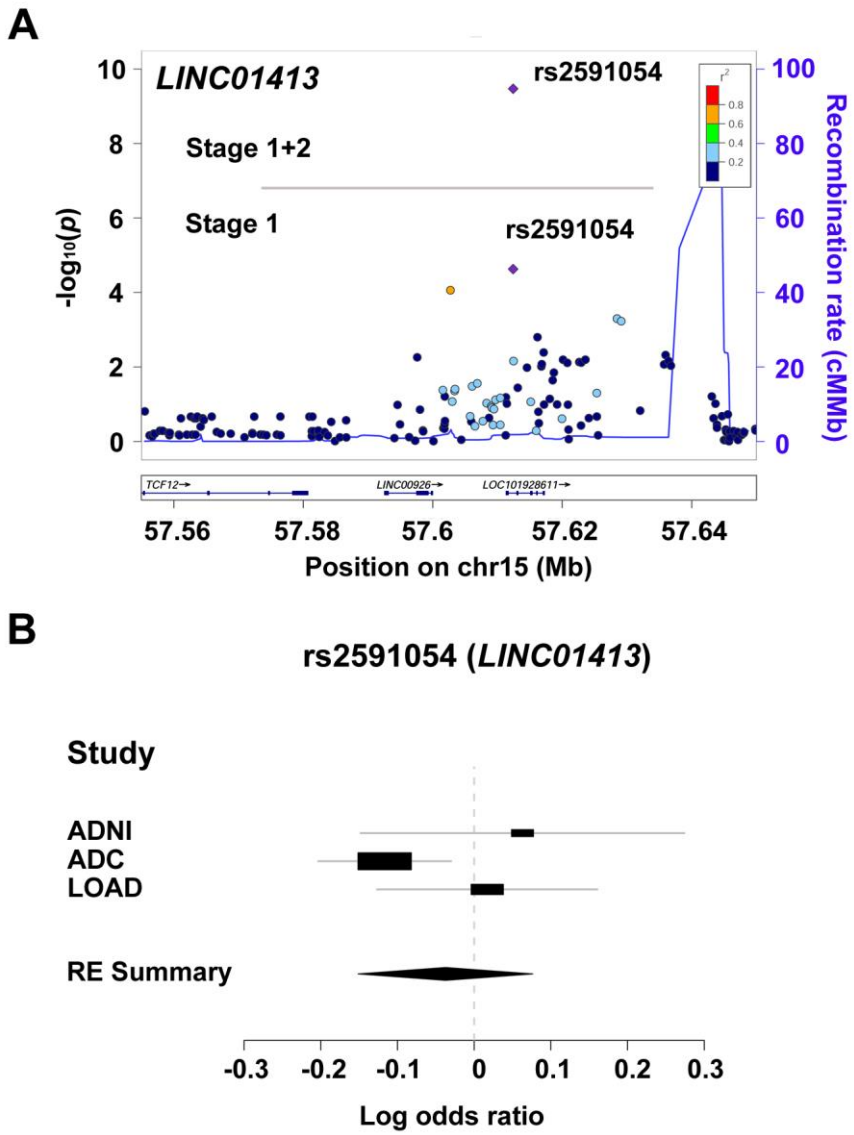

Figure S4. Genetic evidence for the association between *LINC01413* (rs2591054) and AD. (A) Locuszoom plots showing the association results of sentinel variant rs2591054 and other variants in the *LINC01413* locus. The X-axis denotes the genomic coordinate, and the Y-axis denotes the nominal *p*-value in $\log_{10}$ scale. The color map indicates the LD measurement (R^2) for each variant in reference to the sentinel variant (rs2591054, marked by purple diamonds). Signals below and above the grey horizontal line were obtained from the association analysis results from stage 1 and the combined dataset (stage1+2), respectively. (B) Forest plots representing the meta-analysis results of rs2591054 in the three previously published GWAS AD cohorts. Values of effect size (log odds ratio) obtained from independent datasets or meta-results are denoted by squares and diamonds, respectively. For the independent dataset, lines indicate the range of the 95% confidence intervals, and the sizes of squares are proportional to the weights used in the meta-analysis. For the meta-analysis results, the widths of the diamonds cover the range of the 95% confidence intervals. *LINC01413* rs2591054: random effect *p*-value = 5.19E−1, effect size = −0.0375. ADNI (AD: 515, NC: 339), ADC (AD: 3,946, NC: 1,746), and LOAD (AD: 464, NC: 2,231). ADNI, Alzheimer's Disease Neuroimaging Initiative; ADC, Alzheimer's Disease Centers Cohort; LOAD, Late-onset Alzheimer's disease Family Study. RE, random effect.

A

lm(formula = KCNJ15 ~ rs928771 × DX + AGE + PTGENDER + PC1 + PC2 + PC3 + PC4 + PC5)

Coefficients:				
	Estimate	Std. Error	t value	*p*-value
(Intercept)	7.417	0.364	20.398	< 2.00E-16
rs928771	-0.155	0.052	-2.995	2.94E-03
DX_AD	0.362	0.111	3.251	1.27E-03
AGE	0.011	0.005	2.358	1.89E-02
PTGENDER_Male	-0.169	0.062	-2.750	6.28E-03
PC1	-4.385	1.020	-4.297	2.27E-05
PC2	-1.477	1.101	-1.341	1.81E-01
PC3	2.199	1.078	2.041	4.20E-02
PC4	1.966	0.982	2.003	4.60E-02
PC5	1.797	1.808	0.994	3.21E-01
rs928771:DX_AD	-0.128	0.091	-1.408	1.60E-01

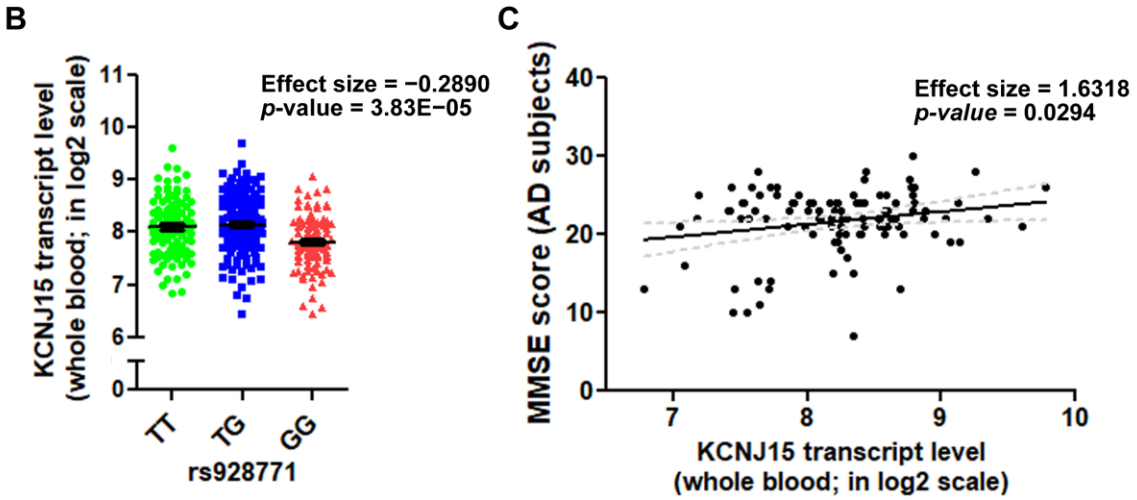

Figure S5. Extended data for genotype- and phenotype-associated modulations of KCNJ15 transcript level in the blood. (A) Table summary for possible effects of interactions between *KCNJ15* rs928771 genotypes and AD. Linear regression model taking the KCNJ15 transcript level as outcome and genotype, phenotype together with the interaction term (genotype×phenotype) as input adjusting for age, gender and top 5 PCs. Model formula: *lm(KCNJ15 ~ rs928771 + phenotype + (rs928771×phenotype) + age + gender +PC[1-5]* (*n* = 244 and 106 for NC and AD subjects, respectively). (B) Association between KCNJ15 transcript level in the blood and KCNJ15 rs928771 genotypes in the MCI subjects (*n* = 101, 164, 104 for MCI subjects harboring zero, one or two copies of rs928771 G alleles); linear regression model, *p*-value = 3.83E–05, effect size = –0.2890. (C) Association between cognitive performance (indicated by Mini-Mental State Examination [MMSE] score) and KCNJ15 rs928771 genotypes in the AD subjects (*n* = 28, 49, 29 for AD subjects harboring zero, one or two copies of rs928771 G allele).

Table S1. Cohort information. A total of 1,222 participants including 489 with AD (*n* = 489), 260 with MCI (*n* = 260), and 473 corresponding age- and gender-matched NCs (*n* = 473) were recruited from Huashan hospital for WGS sequencing. Individuals with a history of neurologic diseases or psychiatric disorders were excluded. Meanwhile, a multicenter control cohort from the CONVERGE study was included for the association analysis (21), and three previously published GWAS AD cohorts (ADNI, ADC, and LOAD) were included for *in silico* replications (22). WGS, whole-genome sequencing; NC, normal control; MCI, mild cognitive impairment; AD, Alzheimer's disease; MMSE, Mini-Mental State Examination; SD, standard deviation; ADNI, Alzheimer's Disease Neuroimaging Initiative; ADC, Alzheimer's Disease Centers Cohort; CONVERGE, China, Oxford and Virginia Commonwealth University Experimental Research on Genetic Epidemiology; LOAD, Late-onset Alzheimer's disease Family Study.

In-house subjects	Participants included for WGS (*n* = 1,222)		
	NC (*n* = 473)	MCI (*n* = 260)	AD (*n* = 489)
Female (%)	249 (53.1%)	122 (47.2%)	263 (53.8%)
Age/years (±SD)	68.2 (±9.2)	69.7 (±7.8)	69.3 (±8.9)
APOE-ε4 carriers (%)	100 (21.1%)	82 (31.5%)	219 (44.8%)
APOE-ε4 frequency Allele number (%)	108 (11.4%)	95 (18.3%)	271 (27.7%)
APOE-ε2 frequency Allele number (%)	77 (8.1%)	32 (6.2%)	34 (3.5%)
MMSE score (±SD)	28.0 (±2.4)	26.4 (±2.0)	14.6 (±6.5)

CONVERGE population controls	All CONVERGE subjects (*n* = 10,640)	CONVERGE elderly controls (Age ≥ 55, *n* =1,745)
Female (%)	100%	100%
Age/years (±SD)	46.0 (±7.6)	57.1 (±1.7)

Previously published GWAS AD cohorts	ADNI	ADC	LOAD	Total number
AD (*n*)	515	3,946	464	4,925
NC (*n*)	339	1,746	2,231	4,316
Female (%)	388 (45.4%)	3,283 (57.6%)	1,680 (62.3%)	
Age/years (±SD)	74.4 (±6.9)	77.8 (±8.3)	81.2 (±10.2)	

Table S2. Quality assessment by comparison with re-sequenced samples (*n* = 126). Site quality assessment was performed by comparing the variant calling of the same individuals from 2 WGS datasets. Two datasets in VCF format (i.e., the whole dataset or the dataset after subgrouping by average DP or MAF) were subjected to *GATK GenotypeConcordance*. Non-reference sensitivity, non-reference discrepancy, and overall genotype concordance were calculated to evaluate sequencing quality. DP, coverage; SNP, single nucleotide polymorphism; MAF, minor allele frequency; SD, standard deviation; WGS, whole-genome sequencing.

Subgrouping of sites by average coverage (DP)

Average DP range	Non-reference sensitivity (SD)	Non-reference discrepancy (SD)	Overall genotype concordance (SD)
DP < 0.5	0.975 (0.002)	0.103 (0.005)	0.905 (0.005)
DP = 0.5–1	0.957 (0.003)	0.150 (0.007)	0.898 (0.005)
DP = 1–2	0.952 (0.003)	0.133 (0.004)	0.922 (0.003)
DP = 2–3	0.973 (0.001)	0.070 (0.002)	0.961 (0.001)
DP = 3–4	0.987 (0.001)	0.036 (0.003)	0.981 (0.002)
DP = 4–5	0.993 (0.001)	0.022 (0.003)	0.988 (0.001)
DP > 5	0.994 (0.001)	0.018 (0.003)	0.991 (0.002)
All	0.989 (0.001)	0.033 (0.003)	0.982 (0.001)

Subgrouping of sites by minor allele frequency (MAF)

MAF range	Non-reference sensitivity (SD)	Non-reference discrepancy (SD)	Overall genotype concordance (SD)
MAF = 0.05–0.1	0.982 (0.001)	0.040 (0.002)	0.989 (0.001)
MAF = 0.1–0.2	0.985 (0.001)	0.038 (0.002)	0.984 (0.001)
MAF = 0.2–0.3	0.990 (0.001)	0.029 (0.003)	0.983 (0.001)
MAF = 0.3–0.4	0.990 (0.001)	0.031 (0.003)	0.978 (0.002)
MAF = 0.4–0.5	0.991 (0.001)	0.033 (0.003)	0.975 (0.002)
All	0.989 (0.001)	0.033 (0.003)	0.982 (0.001)

Table S3. Quality assessment by comparison with genotyping array results (*n* = 96). Site quality assessment was performed by comparing the variant calling in the WGS dataset with an array genotyping dataset from the same individuals. Two datasets in VCF format (i.e., the whole dataset or the dataset after subgrouping by DP or MAF) were subjected to GATK *GenotypeConcordance*. Non-reference sensitivity, non-reference discrepancy, and overall genotype concordance were calculated to evaluate sequencing quality. DP, coverage; SNP, single nucleotide polymorphism; MAF, minor allele frequency; SD, standard deviation WGS, whole-genome sequencing.

Subgrouping of sites by average coverage (DP)

Average DP range	Non-reference sensitivity (SD)	Non-reference discrepancy (SD)	Overall genotype concordance (SD)
DP < 0.5	0.978 (0.066)	0.301 (0.162)	0.779 (0.123)
DP = 0.5–1	0.983 (0.015)	0.075 (0.044)	0.961 (0.026)
DP = 1–2	0.979 (0.008)	0.049 (0.036)	0.978 (0.019)
DP = 2–3	0.981 (0.007)	0.039 (0.034)	0.984 (0.017)
DP = 3–4	0.987 (0.005)	0.029 (0.035)	0.988 (0.017)
DP = 4–5	0.991 (0.003)	0.022 (0.035)	0.991 (0.017)
DP > 5	0.993 (0.003)	0.019 (0.035)	0.992 (0.017)
All	0.991 (0.003)	0.022 (0.034)	0.991 (0.017)

Subgrouping of sites by minor allele frequency (MAF)

MAF range	Non-reference sensitivity (SD)	Non-reference discrepancy (SD)	Overall genotype concordance (SD)
MAF = 0.05–0.1	0.979 (0.009)	0.036 (0.035)	0.994 (0.007)
MAF = 0.1–0.2	0.987 (0.005)	0.027 (0.036)	0.992 (0.012)
MAF = 0.2–0.3	0.991 (0.003)	0.022 (0.036)	0.990 (0.019)
MAF = 0.3–0.4	0.993 (0.002)	0.020 (0.035)	0.988 (0.023)
MAF = 0.4–0.5	0.995 (0.001)	0.019 (0.032)	0.987 (0.026)
All	0.991 (0.003)	0.022 (0.034)	0.991 (0.017)

Table S4. Quality assessment of low-pass sequencing results (*APOE* genotype). The *APOE* genotypes of 1,172 WGS samples were separately generated from low-pass WGS sequencing calls and genotyping using TaqMan assays. Site quality assessment was performed by comparing those 2 datasets (1 individual was removed because of missing records). Overall concordance rate: 0.980; non-reference sensitivity: 0.953; non-reference discrepancy: 0.047. Row: genotypes obtained from WGS dataset; column: genotypes obtained from genotyping. WGS, whole-genome sequencing.

APOE genotype	E2/E2	E2/E3	E2/E4	E3/E3	E3/E4	E4/E4	WGS calls
E2/E2	2	1	0	0	0	0	
E2/E3	1	109	0	2	0	0	
E2/E4	0	2	16	0	0	0	
E3/E3	0	1	1	663	2	0	
E3/E4	0	1	0	8	288	1	
E4/E4	0	0	0	0	4	69	
Genotyping							

Table S5. AD susceptibility variants discovered in the validation stage. Fifty-nine variants passed the validation stage with a nominal *p*-value passing the genome-wide significance threshold ($p < 5E{-}8$) in the combined dataset. AD, Alzheimer's disease; CHR, chromosome(s); BP, base positions in GRCh37 annotation; SNP, single nucleotide polymorphism; EA, effect allele; EAF, effect allele frequency; NC, normal controls; OR, odds ratio. CONVERGE, China, Oxford and Virginia Commonwealth University Experimental Research on Genetic Epidemiology; 1KG: 1000 Genomes Phase 3 cohort; gnomAD, Genome Aggregation Database; EAS, East Asian.

						Stage-1 (AD: 477 NC: 442)			Combined dataset (AD: 477 NC: 2187)			EAF CONVERGE	EAF 1KG EAS	EAF gnomAD EAS
CHR	BP	SNP	Nearest Genes*	EA	EAF_AD	EAF	Nominal *p*-value	OR	EAF	Nominal *p*-value	OR			
14	55297043	rs72713460	GCH1	T	0.160	0.097	5.9E−05	1.77	0.099	4.0E−08	1.74	0.125	0.129	0.120
15	57612410	rs2591054	LINC01413	C	0.683	0.773	1.8E−05	0.64	0.779	3.5E−10	0.61	0.719	0.754	0.755
19	45371168	rs4803766	PVRL2	A	0.468	0.360	2.8E−06	1.56	0.332	3.0E−15	1.76	0.340	0.394	0.386
19	45372794	rs404935	PVRL2	A	0.280	0.154	6.8E−11	2.14	0.145	5.8E−24	2.30	0.144	0.147	0.150
19	45373565	rs395908	PVRL2	A	0.273	0.149	1.2E−10	2.13	0.143	1.9E−22	2.25	0.144	0.144	0.151
19	45376284	rs519113	PVRL2	G	0.297	0.166	4.2E−11	2.12	0.130	3.5E−37	2.83	0.152	0.163	0.168
19	45378144	rs34278513	PVRL2	T	0.262	0.145	5.2E−10	2.10	0.137	9.0E−22	2.24	0.126	0.132	0.147
19	45379516	rs412776	PVRL2	A	0.277	0.146	8.3E−12	2.24	0.136	1.2E−26	2.43	0.129	0.127	0.145
19	45380961	rs3865427	PVRL2	A	0.256	0.137	1.7E−10	2.17	0.128	2.2E−23	2.34	0.125	0.126	0.140
19	45380970	rs11668861	PVRL2	T	0.672	0.775	8.6E−07	0.59	0.794	3.7E−16	0.53	0.787	0.775	0.761
19	45382034	rs6859	PVRL2	G	0.585	0.692	1.7E−06	0.63	0.759	9.7E−28	0.45	0.696	0.692	0.688
19	45382966	rs3852860	PVRL2	T	0.661	0.758	5.5E−06	0.62	0.780	8.4E−15	0.55	0.778	0.765	0.761
19	45383061	rs3852861	PVRL2	T	0.667	0.761	7.5E−06	0.63	0.783	2.0E−14	0.55	0.778	0.765	0.763
19	45383079	rs71352237	PVRL2	C	0.254	0.135	1.4E−10	2.19	0.121	6.0E−26	2.47	0.119	0.124	0.128
19	45383115	rs34224078	PVRL2	G	0.254	0.135	1.4E−10	2.19	0.120	2.2E−26	2.49	0.119	0.124	0.129
19	45383139	rs35879138	PVRL2	A	0.254	0.135	1.4E−10	2.19	0.120	2.2E−26	2.49	0.119	0.124	0.128
19	45387459	rs12972156	PVRL2	G	0.243	0.110	8.8E−14	2.61	0.096	4.5E−36	3.02	0.092	0.095	0.098
19	45387596	rs12972970	PVRL2	A	0.243	0.110	8.8E−14	2.61	0.096	6.4E−36	3.01	0.093	0.095	0.098
19	45388130	rs34342646	PVRL2	A	0.243	0.110	8.8E−14	2.61	0.097	9.1E−36	3.00	0.093	0.095	0.100
19	45388500	rs283811	PVRL2	G	0.312	0.196	1.0E−08	1.87	0.184	9.2E−19	2.01	0.178	0.203	0.194
19	45388568	rs283812	PVRL2	C	0.362	0.231	9.1E−10	1.89	0.165	4.0E−43	2.87	0.156	NA	0.006
19	45390333	rs283815	PVRL2	G	0.319	0.203	1.6E−08	1.84	0.188	3.8E−19	2.02	0.184	0.214	0.194
19	45392254	rs6857	PVRL2	T	0.248	0.111	2.3E−14	2.65	0.096	1.8E−38	3.11	0.094	0.100	0.097
19	45394336	rs71352238	TOMM40	C	0.247	0.109	1.1E−14	2.70	0.096	1.0E−37	3.08	0.094	0.097	0.098
19	45394969	rs184017	TOMM40	G	0.318	0.203	2.1E−08	1.83	0.185	7.8E−20	2.05	0.181	0.208	0.198
19	45395266	rs157580	TOMM40	A	0.550	0.448	1.2E−05	1.51	0.415	2.5E−14	1.72	0.430	0.459	0.443
19	45395619	rs2075650	TOMM40	G	0.245	0.109	2.4E−14	2.67	0.096	2.8E−37	3.07	0.094	0.097	0.087
19	45395714	rs157581	TOMM40	C	0.361	0.236	6.7E−09	1.82	0.208	5.6E−24	2.15	0.220	0.246	0.228
19	45395909	rs34404554	TOMM40	G	0.246	0.109	1.6E−14	2.68	0.096	1.0E−37	3.09	0.094	0.097	0.099
19	45396144	rs11556505	TOMM40	T	0.245	0.108	1.4E−14	2.70	0.096	2.8E−37	3.07	0.094	0.096	0.087
19	45396219	rs157582	TOMM40	T	0.322	0.204	9.7E−09	1.86	0.188	5.7E−20	2.05	0.182	0.209	0.186
19	45396665	rs59007384	TOMM40	T	0.321	0.215	3.3E−07	1.73	0.184	4.6E−21	2.09	0.189	0.227	0.208
19	45404691	rs405697	TOMM40	G	0.512	0.411	1.5E−05	1.50	0.387	1.3E−12	1.66	0.392	0.436	0.418
19	45406673	rs10119	TOMM40	A	0.280	0.119	8.8E−18	2.88	0.098	1.7E−51	3.57	0.097	0.096	0.102
19	45409167	rs440446	APOE	G	0.508	0.407	1.4E−05	1.51	0.381	4.3E−13	1.68	0.383	0.428	0.396
19	45410002	rs769449	APOE	A	0.252	0.104	2.2E−16	2.89	0.089	8.1E−45	3.42	0.086	0.077	0.090
19	45411941	rs429358	APOE	C	0.278	0.113	9.5E−19	3.02	0.083	4.1E−64	4.25	0.093	0.086	0.089
19	45413576	rs75627662	APOE	T	0.306	0.200	2.0E−07	1.76	0.191	3.4E−15	1.87	0.185	0.191	0.189
19	45414451	rs439401	APOE	C	0.535	0.427	3.6E−06	1.55	0.407	4.9E−13	1.68	0.407	0.444	0.414
19	45415713	rs10414043	Intergenic	A	0.269	0.114	4.8E−17	2.86	0.108	2.4E−39	3.04	0.104	0.088	0.100
19	45415935	rs7256200	APOC1	T	0.266	0.114	1.6E−16	2.81	0.107	6.6E−39	3.04	0.104	0.085	0.097
19	45416178	rs483082	APOC1	T	0.332	0.207	1.6E−09	1.91	0.195	1.4E−20	2.06	0.191	0.202	0.193
19	45416478	rs584007	APOC1	G	0.531	0.429	1.1E−05	1.51	0.402	2.8E−13	1.69	0.407	0.447	0.416
19	45416741	rs438811	APOC1	T	0.332	0.207	1.6E−09	1.91	0.195	1.4E−20	2.06	0.192	0.202	0.194
19	45418790	rs5117	APOC1	C	0.308	0.201	1.6E−07	1.77	0.185	2.0E−17	1.96	0.181	0.205	0.189
19	45418961	rs3826688	APOC1	C	0.531	0.430	1.3E−05	1.50	0.402	2.8E−13	1.69	0.397	0.454	0.422

19	45420082	rs73052335	APOC1	C	0.325	0.153	7.1E−18	2.67	0.101	3.5E−72	4.27	0.112	NA	0.094
19	45421254	rs12721046	APOC1	A	0.296	0.126	6.5E−19	2.92	0.105	1.8E−53	3.57	0.116	0.097	0.111
19	45421877	rs484195	APOC1	G	0.533	0.424	3.4E−06	1.55	0.396	8.1E−15	1.74	0.404	0.460	0.416
19	45422160	rs12721051	APOC1	G	0.296	0.127	1.2E−18	2.89	0.118	2.1E−44	3.15	0.116	0.099	0.098
19	45422846	rs56131196	APOC1	A	0.297	0.127	7.8E−19	2.91	0.117	2.4E−45	3.19	0.116	0.099	0.113
19	45422946	rs4420638	APOC1	G	0.293	0.127	4.1E−18	2.85	0.118	4.8E−43	3.10	0.116	0.099	0.114
19	45425175	rs157594	Intergenic	G	0.533	0.427	5.5E−06	1.53	0.393	2.0E−15	1.76	0.336	0.454	0.415
19	45425460	rs157595	Intergenic	G	0.535	0.428	4.5E−06	1.54	0.396	3.5E−15	1.75	0.399	0.463	0.414
19	45427125	rs111789331	Intergenic	A	0.269	0.121	1.5E−15	2.68	0.113	1.4E−36	2.91	0.112	0.092	0.104
19	45428234	rs66626994	APOC1P1	A	0.270	0.122	1.8E−15	2.66	0.112	3.7E−37	2.93	0.108	0.091	0.105
19	45429708	rs60049679	APOC1P1	C	0.245	0.154	1.0E−06	1.79	0.109	2.0E−29	2.67	0.115	0.129	0.151
21	39663760	rs928771	KCNJ15	G	0.238	0.154	6.0E−06	1.72	0.161	1.2E−08	1.63	0.172	0.125	0.172
21	39664976	rs2836293	KCNJ15	A	0.235	0.154	1.2E−05	1.69	0.161	4.5E−08	1.60	0.172	0.125	0.172

358 * For the *APOE* region, the nearest genes located within ±2 kb of the listed SNPs
359

Table S6. Examination of covariates effects in stage 1 analysis. Commonly used covariates in the genome-wide association study, including age, gender, and principal components, were tested in the stage 1 analysis. Upper panel: statistical metrics of Spearman's correlation test between the newly identified candidate alleles and covariates (i.e., age and gender) in stage 1 subjects (n = 442 and 477, for NC and AD respectively). Lower panel: logistic regression of the risk effects of the variants with or without adjustment for principal components (the top five that were phenotype-independent), age, and gender (n = 442, 477 for NC and AD, respectively). Rho, Spearman's rank correlation coefficient; PC, principal components; SE, standard error; OR, odds ratio.

Gene	Variant	Age		Gender	
		Rho	*p*-value	Rho	*p*-value
GCH1	14:55297043_T	−0.0055	0.8677	−0.0619	0.0604
LINC01413	15:57612410_C	−0.0573	0.0821	−0.0332	0.3142
KCNJ15	21:39663760_G	−0.0137	0.6779	0.0104	0.7513

Gene	Variant	*p*-value (unadjusted)	*p*-value (age+gender)	*p*-value (top 5 PCs +age+gender)	Effect size	SE	OR
GCH1	14:55297043_T	6.93E−05	6.53E−05	6.31E−05	0.5877	0.1469	1.80
LINC01413	15:57612410_C	2.59E−05	3.80E−05	3.50E−05	−0.4507	0.1089	0.64
KCNJ15	21:39663760_G	2.25E−05	1.91E−05	9.81E−06	0.5371	0.1215	1.71

Table S7. Examination of covariates effects in stage 1+2 analysis. Commonly used covariates in the genome-wide association study, including age, gender, and batch effects were tested in the stage 1+2 analysis. Upper panel: Spearman's correlation test between the newly identified candidate alleles and covariates (i.e., age, gender, and batch effects) in stage 1+2 control subjects, which comprised both in-house controls (n = 442) and CONVERGE elderly controls (n = 1,745). Lower panel: summary metrics for logistic regression before and after adjusting age and gender as covariates. Rho, Spearman's rank correlation coefficient; SE, standard error; OR, odds ratio.

Gene	Variant	Age		Gender		Batch	
		Rho	*p*-value	Rho	*p*-value	Rho	*p*-value
GCH1	14:55297043_T	−0.0146	0.4953	−0.0259	0.2259	−0.0043	0.8395
LINC01413	15:57612410_C	−0.0130	0.5434	−0.0077	0.7188	0.0134	0.5308
KCNJ15	21:39663760_G	−0.0176	0.4110	0.0127	0.5519	0.0138	0.5189

Gene	Variant	*p*-value (unadjusted)	*p*-value (age+gender)	Effect size	SE	OR
GCH1	14:55297043_T	1.55E−07	1.49E−05	0.5199	0.1201	1.68
LINC01413	15:57612410_C	8.89E−10	2.45E−06	−0.4463	0.0947	0.64
KCNJ15	21:39663760_G	9.21E−08	5.99E−07	0.5139	0.1030	1.67

Table S8. Correction for population stratification in stage 1+2 analysis. Summary metrics of the association results before and after adjustment for population stratification. Upper panel: summary metrics after application of the genetic similarity score matching (GSM) method with the conditional logistic regression model before and after adjustment for age and gender. Lower panel: summary metrics for logistic regression after inclusion of phenotype-associated principal components (PC1 and PC3, at a nominal level of $p < 0.05$), with further adjustment for age and gender. GSM, genetic similarity score matching; SE, standard error; OR, odds ratio; PC, principal component.

Gene	Variant	*p*-value (unadjusted)	*p*-value (GSM)	Effect size	SE	OR	*p*-value (GSM +age+gender)	Effect size	SE	OR
GCH1	14:55297043_T	1.55E−07	2.45E−07	0.5214	0.1010	1.684	1.55E−04	0.5046	0.1334	1.657
LINC01413	15:57612410_C	8.89E−10	3.68E−10	−0.5042	0.0804	0.604	3.32E−05	−0.4197	0.1011	0.657
KCNJ15	21:39663760_G	9.21E−08	3.23E−08	0.4866	0.0880	1.627	1.49E−06	0.5385	0.1119	1.714

Gene	Variant	*p*-value (unadjusted)	*p*-value (PC 1, 3)	Effect size	SE	OR	*p*-value (PC 1, 3 +age+gender)	Effect size	SE	OR
GCH1	14:55297043_T	1.55E−07	4.42E−05	0.5910	0.1447	1.806	4.36E−05	0.5944	0.1454	1.81
LINC01413	15:57612410_C	8.89E−10	2.21E−05	−0.4578	0.1079	0.633	3.65E−05	−0.4467	0.1082	0.64
KCNJ15	21:39663760_G	9.21E−08	4.22E−06	0.5487	0.1193	1.731	3.60E−06	0.5552	0.1198	1.74

Table S9. Summary for AD susceptibility variants after adjusting for confounding factors. Statistical metrics for fifty-nine variants passed the validation stage with a nominal *p*-value passing the genome-wide significance threshold ($p < 5E{-}8$) in the combined dataset after adjusting for age, gender and phenotype-associated PCs. AD, Alzheimer's disease; CHR, chromosome(s); BP, base positions in GRCh37 annotation; SNP, single nucleotide polymorphism; EA, effect allele; EAF, effect allele frequency; NC, normal controls; OR, odds ratio. CONVERGE, China, Oxford and Virginia Commonwealth University Experimental Research on Genetic Epidemiology; 1KG: 1000 Genomes Phase 3 cohort; gnomAD, Genome Aggregation Database; EAS, East Asian.

						Stage-1 (AD: 477 NC: 442)			Combined dataset (AD: 477 NC: 2187)			EAF CONVERGE	EAF 1KG EAS	EAF gnomAD EAS
CHR	BP	SNP	Nearest Genes*	EA	EAF_AD	EAF	Effect size	*p*-value	EAF	Effect size	*p*-value			
14	55297043	rs72713460	GCH1	T	0.160	0.097	0.588	6.31E−05	0.099	0.595	4.36E−05	0.125	0.129	0.120
15	57612410	rs2591054	LINC01413	C	0.683	0.773	0.451	3.50E−05	0.779	0.447	3.65E−05	0.719	0.754	0.755
19	45371168	rs4803766	PVRL2	A	0.468	0.360	0.428	6.71E−06	0.332	0.424	7.96E−06	0.340	0.394	0.386
19	45372794	rs404935	PVRL2	A	0.280	0.154	0.722	7.11E−10	0.145	0.715	7.55E−10	0.144	0.147	0.150
19	45373565	rs395908	PVRL2	A	0.273	0.149	0.731	9.11E−10	0.143	0.728	7.66E−10	0.144	0.144	0.151
19	45376284	rs519113	PVRL2	G	0.297	0.166	0.745	1.87E−10	0.130	0.759	7.02E−11	0.152	0.163	0.168
19	45378144	rs34278513	PVRL2	T	0.262	0.145	0.720	2.88E−09	0.137	0.709	3.46E−09	0.126	0.132	0.147
19	45379516	rs412776	PVRL2	A	0.277	0.146	0.778	9.82E−11	0.136	0.766	1.29E−10	0.129	0.127	0.145
19	45380961	rs3865427	PVRL2	A	0.256	0.137	0.731	1.87E−09	0.128	0.724	1.90E−09	0.125	0.126	0.140
19	45380970	rs11668861	PVRL2	T	0.672	0.775	0.518	1.31E−06	0.794	0.500	2.61E−06	0.787	0.775	0.761
19	45382034	rs6859	PVRL2	G	0.585	0.692	0.515	6.72E−07	0.759	0.509	7.43E−07	0.696	0.692	0.688
19	45382966	rs3852860	PVRL2	T	0.661	0.758	0.481	6.13E−06	0.780	0.457	1.52E−05	0.778	0.765	0.761
19	45383061	rs3852861	PVRL2	T	0.667	0.761	0.470	9.26E−06	0.783	0.447	2.26E−05	0.778	0.765	0.763
19	45383079	rs71352237	PVRL2	C	0.254	0.135	0.746	1.49E−09	0.121	0.734	1.81E−09	0.119	0.124	0.128
19	45383115	rs34224078	PVRL2	G	0.254	0.135	0.746	1.49E−09	0.120	0.734	1.78E−09	0.119	0.124	0.129
19	45383139	rs35879138	PVRL2	A	0.254	0.135	0.746	1.49E−09	0.120	0.734	1.78E−09	0.119	0.124	0.128
19	45387459	rs12972156	PVRL2	G	0.243	0.110	0.913	4.96E−12	0.096	0.897	5.95E−12	0.092	0.095	0.098
19	45387596	rs12972970	PVRL2	A	0.243	0.110	0.913	4.96E−12	0.096	0.897	5.97E−12	0.093	0.095	0.098
19	45388130	rs34342646	PVRL2	A	0.243	0.110	0.913	4.96E−12	0.097	0.897	5.98E−12	0.093	0.095	0.100
19	45388500	rs283811	PVRL2	G	0.312	0.196	0.623	2.82E−08	0.184	0.590	1.22E−07	0.178	0.203	0.194
19	45388568	rs283812	PVRL2	C	0.362	0.231	0.532	4.82E−08	0.165	0.519	1.04E−07	0.156	NA	0.006
19	45390333	rs283815	PVRL2	G	0.319	0.203	0.609	4.25E−08	0.188	0.576	1.96E−07	0.184	0.214	0.194
19	45392254	rs6857	PVRL2	T	0.248	0.111	0.919	2.21E−12	0.096	0.900	3.27E−12	0.094	0.100	0.097
19	45394336	rs71352238	TOMM40	C	0.247	0.109	0.934	1.25E−12	0.096	0.917	1.67E−12	0.094	0.097	0.098
19	45394969	rs184017	TOMM40	G	0.318	0.203	0.605	4.66E−08	0.185	0.572	2.07E−07	0.181	0.208	0.198
19	45395266	rs157580	TOMM40	A	0.550	0.448	0.404	1.99E−05	0.415	0.381	5.53E−05	0.430	0.459	0.443
19	45395619	rs2075650	TOMM40	G	0.245	0.109	0.933	1.84E−12	0.096	0.918	2.06E−12	0.094	0.097	0.087
19	45395714	rs157581	TOMM40	C	0.361	0.236	0.587	2.19E−08	0.208	0.564	7.06E−08	0.220	0.246	0.228
19	45395909	rs34404554	TOMM40	G	0.246	0.109	0.934	1.53E−12	0.096	0.920	1.65E−12	0.094	0.097	0.099
19	45396144	rs11556505	TOMM40	T	0.245	0.108	0.939	1.36E−12	0.096	0.926	1.36E−12	0.094	0.096	0.087
19	45396219	rs157582	TOMM40	T	0.322	0.204	0.607	2.86E−08	0.188	0.578	1.13E−07	0.182	0.209	0.186
19	45396665	rs59007384	TOMM40	T	0.321	0.215	0.538	7.00E−07	0.184	0.503	3.21E−06	0.189	0.227	0.208
19	45404691	rs405697	TOMM40	G	0.512	0.411	0.406	2.14E−05	0.387	0.392	4.20E−05	0.392	0.436	0.418
19	45406673	rs10119	TOMM40	A	0.280	0.119	0.999	3.73E−15	0.098	0.980	5.10E−15	0.097	0.096	0.102
19	45409167	rs440446	APOE	G	0.508	0.407	0.401	2.58E−05	0.381	0.378	7.20E−05	0.383	0.428	0.396
19	45410002	rs769449	APOE	A	0.252	0.104	0.984	1.09E−13	0.089	0.950	2.75E−13	0.086	0.077	0.090
19	45411941	rs429358	APOE	C	0.278	0.113	1.013	2.23E−15	0.083	0.991	3.77E−15	0.093	0.086	0.089
19	45413576	rs75627662	APOE	T	0.306	0.200	0.526	1.00E−06	0.191	0.506	2.34E−06	0.185	0.191	0.189
19	45414451	rs439401	APOE	C	0.535	0.427	0.429	7.32E−06	0.407	0.406	2.13E−05	0.407	0.444	0.414
19	45415713	rs10414043	Intergenic	A	0.269	0.114	0.974	3.13E−14	0.108	0.940	8.48E−14	0.104	0.088	0.100
19	45415935	rs7256200	APOC1	T	0.266	0.114	0.961	7.38E−14	0.107	0.926	1.96E−13	0.104	0.085	0.097
19	45416178	rs483082	APOC1	T	0.332	0.207	0.602	1.52E−08	0.195	0.583	4.06E−08	0.191	0.202	0.193
19	45416478	rs584007	APOC1	G	0.531	0.429	0.406	2.08E−05	0.402	0.382	6.09E−05	0.407	0.447	0.416
19	45416741	rs438811	APOC1	T	0.332	0.207	0.602	1.52E−08	0.195	0.583	4.07E−08	0.192	0.202	0.194
19	45418790	rs5117	APOC1	C	0.308	0.201	0.522	1.03E−06	0.185	0.500	2.73E−06	0.181	0.205	0.189

19	45418961	rs3826688	APOC1	C	0.531	0.430	0.403	2.52E−05	0.402	0.380	6.97E−05	0.397	0.454	0.422
19	45420082	rs73052335	APOC1	C	0.325	0.153	0.877	1.30E−14	0.101	0.870	1.44E−14	0.112	NA	0.094
19	45421254	rs12721046	APOC1	A	0.296	0.126	0.986	1.26E−15	0.105	0.964	2.10E−15	0.116	0.097	0.111
19	45421877	rs484195	APOC1	G	0.533	0.424	0.437	6.11E−06	0.396	0.410	2.07E−05	0.404	0.460	0.416
19	45422160	rs12721051	APOC1	G	0.296	0.127	0.976	1.96E−15	0.118	0.949	4.46E−15	0.116	0.099	0.098
19	45422846	rs56131196	APOC1	A	0.297	0.127	0.982	1.37E−15	0.117	0.957	2.77E−15	0.116	0.099	0.113
19	45422946	rs4420638	APOC1	G	0.293	0.127	0.968	4.05E−15	0.118	0.940	9.07E−15	0.116	0.099	0.114
19	45425175	rs157594	Intergenic	G	0.533	0.427	0.432	8.38E−06	0.393	0.405	2.78E−05	0.336	0.454	0.415
19	45425460	rs157595	Intergenic	G	0.535	0.428	0.434	7.14E−06	0.396	0.406	2.54E−05	0.399	0.463	0.414
19	45427125	rs111789331	Intergenic	A	0.269	0.121	0.920	3.14E−13	0.113	0.892	6.74E−13	0.112	0.092	0.104
19	45428234	rs66626994	APOC1P1	A	0.270	0.122	0.919	3.08E−13	0.112	0.894	5.86E−13	0.108	0.091	0.105
19	45429708	rs60049679	APOC1P1	C	0.245	0.154	0.559	3.39E−06	0.109	0.528	1.16E−05	0.115	0.129	0.151
21	39663760	rs928771	KCNJ15	G	0.238	0.154	0.537	9.81E−06	0.161	0.555	3.60E−06	0.172	0.125	0.172
21	39664976	rs2836293	KCNJ15	A	0.235	0.154	0.537	9.81E−06	0.161	0.555	3.60E−06	0.172	0.125	0.172

410 * For the *APOE* region, the nearest genes located within ±2 kb of the listed SNPs
411

Table S10. Transethnic meta-analysis of identified AD risk loci. Three previously published GWAS AD cohorts with cases diagnoses of AD and healthy normal controls together with the Chinese dataset were included in the meta-analysis: ADNI (AD: 515, NC: 339), ADC (AD: 3,946, NC: 1,746), LOAD (AD: 464, NC: 2,231), and the combined dataset for the Chinese population (AD: 477, NC: 2,187). Meta *p*-values were obtained from the METASOFT program on the basis of the estimation of the Han and Eskin's Random Effects model (RE-HE, or RE2). AD, Alzheimer's disease; CHR, chromosome(s); BP, base positions in GRCh37 annotation; SNP, single nucleotide polymorphism; EA, effect alleles; EAF, effect allele frequency; OR, odds ratio; SD, standard deviations; NC, normal control; WGS, whole-genome sequencing; ADNI, Alzheimer's Disease Neuroimaging Initiative; ADC, Alzheimer's Disease Centers Cohort; LOAD, Late-onset Alzheimer's disease Family Study; I^2, *I*-square heterogeneity statistic; *Q*, Cochrane's *Q* statistic; τ^2, *Tau*-square heterogeneity estimator of DerSimonian–Laird.

Variants	Genes	Cohorts	*p*-value	Effect size	SE	*p*-value	I^2	*Q*	*p*-value (*Q*)	τ^2
rs72713460*	GCH1	Chinese	4.36E−05	0.5944	0.1454	2.53E–04	73.81	11.46	9.50E–03	0.024
		ADNI	9.60E−02	0.2154	0.1294					
		ADC	1.44E−01	0.0788	0.0539					
		LOAD	1.64E−01	0.1181	0.0849					
rs928771*	KCNJ15	Chinese	3.60E−06	0.5552	0.1198	6.41E–04	81.31	16.05	1.11E–03	0.026
		ADNI	7.44E−01	0.0338	0.1035					
		ADC	1.93E−01	0.0574	0.0441					
		LOAD	4.11E−01	0.0607	0.0738					

* Statistical metrics with $p < 5E{-}2$ in the corresponding cohort(s).

Table S11. Plasma biomarkers associated with AD risk genotypes. A total of 146 plasma biomarkers obtained from the ADNI dataset were included in the analysis of possible modulation effects due to the identified AD risk variants, rs72713460 and rs928771. Ten biomarkers exhibiting low variance in their expression levels were removed prior to the analysis. The table shows the plasma biomarkers significantly associated with the genotypes in the AD subjects (sample $n = 69$) with a $p < 0.05$ after adjusting for age, gender, and the top five PCs. Biomarkers with an average detection signal lower than the limit of detection (LOD) were also excluded from the table. SE, standard error; FDR, false discovery rate.

Gene	SNP	Biomarker	Effect size	SE	*p*-value	FDR
GCH1	**rs72713460**	Matrix metalloproteinase-2 (MMP-2) (ng/mL)	0.0534	0.0176	3.07E−03	0.276
		Pancreatic polypeptide (PPP) (pg/mL)	−0.1454	0.0541	8.50E−03	0.459
		Eotaxin-3 (pg/mL)	−0.0476	0.0200	1.93E−02	0.579
		Matrix petalloproteinase-7 (MMP-7) (ng/mL)	0.0566	0.0248	2.48E−02	0.604
		Resistin (ng/mL)	0.0360	0.0160	2.69E−02	0.604
		Glutathione S-transferase alpha (GST-alpha) (ng/mL)	−0.1305	0.0637	4.32E−02	0.729
KCNJ15	**rs928771**	TNF-related apoptosis-inducing ligand receptor 3 (TRAIL-R3) (ng/mL)	−0.0553	0.0174	2.00E−03	0.276
		Alpha-1-microglobulin (A1Micro) (μg/mL)	−0.0451	0.0144	2.30E−03	0.276
		Tissue inhibitor of metalloproteinases-1 (TIMP-1) (ng/mL)	−0.0364	0.0149	1.65E−02	0.556
		Myeloid progenitor inhibitory factor-1 (CCL23) (ng/mL)	−0.0298	0.0131	2.59E−02	0.604
		Thrombomodulin (TM) (ng/mL)	−0.0319	0.0145	2.99E−02	0.605
		Apolipoprotein H (Apo H) (μg/mL)	−32.2527	14.7603	3.14E−02	0.605
		Thymus-expressed chemokine (TECK) (ng/mL)	−0.0420	0.0207	4.50E−02	0.729
		Macrophage-derived chemokine (MDC) (pg/mL)	−0.0323	0.0160	4.59E−02	0.729
		Brain-derived neurotrophic factor (BDNF) (ng/mL)	0.0959	0.0480	4.86E−02	0.729

Table S12. CSF biomarkers associated with AD risk genotypes. A total of 83 plasma biomarkers obtained from the ADNI dataset were included in the analysis of possible modulation effects due to the identified AD risk variants, rs72713460 and rs928771. One biomarker exhibiting low variance in its expression level was removed prior to the analysis. The table shows the plasma biomarkers significantly associated with the genotypes in the AD subjects (sample $n = 103$) with a $p < 0.05$ after adjusting for age, gender, and the top five PCs. Biomarkers with an average detection signal lower than the limit of detection (LOD) were also excluded from the table. SE, standard error; FDR, false discovery rate.

Gene	SNP	Biomarker	Effect size	SE	*p*-value	FDR
GCH1	rs72713460	Interleukin-25 (IL-25) (pg/mL)	−0.9062	0.4089	3.05E−02	0.973
		Angiotensin-converting enzyme (ACE) (ng/mL)	−0.0648	0.0299	3.43E−02	0.973
		Immunoglobulin A (IgA) (mg/mL)	0.0920	0.0426	3.48E−02	0.973
		C-reactive protein (CRP）(μg/mL)	0.2424	0.1165	4.18E−02	0.973
KCNJ15	rs928771	Cancer antigen 19-9 (U/mL)	0.1511	0.0592	1.33E−02	0.973
		Interleukin-25 (IL-25) (pg/mL)	1.0349	0.4843	3.67E−02	0.973
		Macrophage colony-stimulating factor-1 (M-CSF) (ng/mL)	0.0569	0.0282	4.84E−02	0.986

Table S13. GO analysis of the genes regulated by AD susceptibility loci. A total of 52 candidate variants from 3 AD susceptibility loci (*APOE-APOC1*, 49 SNPs; *KCNJ15*, 2 SNPs; and *GCH1* 1 SNP) passing the genome-wide significance threshold in the combined dataset were subjected to genotype-expression analysis for possible regulatory effects in the hippocampal and blood transcriptome datasets (GTEx dataset). The table shows the representative ontologies for identified genes regulated by AD risk loci obtained from blood (sample n = 365) and hippocampus (sample n = 87) transcriptome datasets with an FDR < 1E−3. GO, gene ontology; FDR, false discovery rate.

Blood eGene network			
Pathway ID	Description	Counts	FDR
GO.0006952	Defense response	27	3.61E−06
GO.0006955	Immune response	25	1.19E−05
GO.0045087	Innate immune response	21	1.32E−05
GO.0006950	Response to stress	39	1.07E−04
GO.0002376	Immune system process	28	2.04E−04
GO.0006956	Complement activation	6	2.04E−04
GO.0002460	Adaptive immune response based on somatic recombination of immune receptors built from immunoglobulin superfamily domains	8	2.23E−04
GO.0050776	Regulation of immune response	17	4.72E−04
GO.0006958	Complement activation, classical pathway	5	6.46E−04
GO.0050778	Positive regulation of immune response	14	6.46E−04
Hippocampus eGene network			
Pathway ID	Description	Counts	FDR
GO.0071310	Cellular response to organic substance	44	6.69E−10
GO.0010033	Response to organic substance	48	1.05E−08
GO.0016032	Viral process	26	1.05E−08
GO.0044403	Symbiosis, encompassing mutualism through parasitism	27	1.05E−08
GO.0070887	Cellular response to chemical stimulus	46	1.05E−08
GO.0007166	Cell surface receptor signalling pathway	41	2.02E−07
GO.0007165	Signal transduction	65	2.39E−07
GO.0071363	Cellular response to growth factor stimulus	22	6.93E−07
GO.0044700	Single organism signalling	65	2.63E−06
GO.0009719	Response to endogenous stimulus	31	3.89E−06
GO.0051128	Regulation of cellular component organization	39	4.92E−06
GO.0007154	Cell communication	64	1.44E−05
GO.0006950	Response to stress	50	1.81E−05
GO.0071345	Cellular response to cytokine stimulus	18	2.00E−05
GO.0051704	Multi-organism process	38	2.86E−05
GO.0009611	Response to wounding	21	3.84E−05
GO.0051130	Positive regulation of cellular component organization	26	3.90E−05
GO.0034097	Response to cytokine	19	4.51E−05
GO.0051716	Cellular response to stimulus	69	5.12E−05
GO.0071495	Cellular response to endogenous stimulus	24	5.73E−05
GO.0051641	Cellular localization	36	5.99E−05
GO.0042221	Response to chemical	51	6.63E−05
GO.0048522	Positive regulation of cellular process	56	7.54E−05
GO.0010941	Regulation of cell death	29	7.91E−05
GO.0006952	Defence response	28	9.98E−05
GO.0019058	Viral life cycle	12	9.98E−05
GO.0007167	Enzyme linked receptor protein signalling pathway	22	1.47E−04
GO.0019222	Regulation of metabolic process	70	2.00E−04
GO.0042981	Regulation of apoptotic process	27	2.13E−04
GO.0048583	Regulation of response to stimulus	46	2.13E−04
GO.1902531	Regulation of intracellular signal transduction	27	2.22E−04
GO.0045667	Regulation of osteoblast differentiation	8	3.86E−04

GO.0045087	Innate immune response	21	5.55E−04
GO.2001137	Positive regulation of endocytic recycling	3	5.55E−04
GO.0051649	Establishment of localization in cell	30	5.84E−04
GO.0014070	Response to organic cyclic compound	19	7.73E−04
GO.0034613	Cellular protein localization	23	7.73E−04
GO.0008104	Protein localization	29	7.80E−04
GO.0050793	Regulation of developmental process	33	7.80E−04
GO.0009653	Anatomical structure morphogenesis	33	7.85E−04
GO.0007507	Heart development	14	8.99E−04
GO.0060429	Epithelium development	21	8.99E−04
GO.0051246	Regulation of protein metabolic process	36	9.01E−04
GO.0005829	Cytosol	56	1.21E−08
GO.0005925	Focal adhesion	13	7.21E−04
GO.0043233	Organelle lumen	53	7.21E−04
GO.0070013	Intracellular organelle lumen	52	7.21E−04
4510	Focal adhesion	11	9.16E−05

458

Table S14. Summary statistics for the Caucasian AD risk loci in the Chinese population. Detailed summary statistics for the 16 AD Caucasian risk loci (23) in Chinese subjects (AD: 477; NC: 2187 [442 from the in-house WGS dataset and 1,745 from CONVERGE dataset]) derived from the association analysis results based on the Chinese WGS dataset. EA, effect allele; EAF, effect allele frequency in the combined control samples; OR, odds ratio; CI, confidence intervals; WGS, whole-genome sequencing. CONVERGE, China, Oxford and Virginia Commonwealth University Experimental Research on Genetic Epidemiology; 1KG: 1000 Genomes Phase 3 cohort; gnomAD, Genome Aggregation Database; EAS, East Asian. β, beta (effect size); SE, standard error; OR, odds ratio.

SNPs	Location	Genes	EA	Caucasian GWAS			Chinese WGS data (Adjusted for age, gender, and phenotype-associated PCs)					EAF in CONVERGE	EAF in 1KG (EAS)	EAF in gnomAD (EAS)
				EAF	*p*-value	OR	EAF	*p*-value	*β*	SE	OR			
rs6733839*	2:127892810	BIN1	T	0.409	6.9E−44	1.21	0.453	4.7E−02	0.188	0.094	1.21	0.444	0.372	0.437
rs190982	5:88223420	MEF2C	G	0.408	3.2E−08	0.92	0.128	3.8E−01	0.118	0.136	1.13	0.157	0.133	0.149
rs9271192	6:32578530	HLA-DRB5 HLA-DRB1	C	0.276	5.2E−11	1.11	0.182	8.6E−01	0.022	0.128	1.02	0.197	0.231	0.188
rs10948363*	6:47487762	CD2AP	G	0.266	2.9E−12	1.10	0.123	4.5E−02	0.286	0.143	1.33	0.122	0.123	0.148
rs2718058	7:37841534	NME8	G	0.373	1.1E−13	1.10	0.218	8.3E−01	0.024	0.113	1.02	0.216	0.191	0.201
rs1476679	7:100004446	ZCWPW1	C	0.287	4.8E−09	0.93	0.371	9.7E−01	0.019	0.101	1.02	0.329	0.349	0.333
rs11771145†	7:143110762	EPHA1	A	0.338	5.6E−10	0.92	0.546	1.4E−01	−0.135	0.092	0.87	0.522	0.522	0.496
rs28834970	8:27195121	PTK2B	C	0.366	2.8E−25	0.90	0.273	7.0E−01	0.039	0.101	1.04	0.265	0.257	0.305
rs9331896	8:27467686	CLU	C	0.379	7.4E−14	1.10	0.186	8.4E−01	0.024	0.120	1.02	0.195	0.219	0.205
rs10838725	11:47557871	CELF1	C	0.316	6.1E−16	0.86	0.313	5.1E−01	0.068	0.102	1.07	0.303	0.386	0.374
rs10792832	11:85867875	PICALM	A	0.358	9.7E−15	1.08	0.381	7.4E−02	−0.174	0.098	0.84	0.382	0.409	0.408
rs11218343	11:121435587	SORL1	C	0.039	1.1E−08	0.88	0.311	1.1E−01	−0.169	0.107	0.84	0.282	0.288	0.294
rs17125944*	14:53400629	FERMT2	C	0.092	5.5E−09	0.76	0.229	3.6E−02	−0.240	0.114	0.79	0.224	0.227	0.211
rs10498633	14:92926952	SLC24A4-RIN3	T	0.217	7.9E−09	1.13	0.111	9.1E−01	−0.018	0.157	0.98	0.113	0.085	0.100
rs4147929	19:1063443	ABCA7	A	0.190	1.1E−15	0.90	0.329	1.5E−01	0.140	0.098	1.15	0.326	0.354	0.334
rs3865444	19:51727962	CD33	A	0.307	3.0E−06	1.14	0.191	8.1E−01	0.030	0.126	1.03	0.191	0.186	0.175

* Statistical metrics with $p < 5E{-}2$ in the Chinese dataset.

† Minor allele switched in Chinese cohort (EPHA1, rs11771145).

Caucasian GWAS data were obtained from ref. 23.

Supplemental References

1. Saykin AJ, *et al.* (2015) Genetic studies of quantitative MCI and AD phenotypes in ADNI: Progress, opportunities, and plans. *Alzheimers Dement* 11(7):792-814.

2. Naj AC, *et al.* (2011) Common variants at MS4A4/MS4A6E, CD2AP, CD33 and EPHA1 are associated with late-onset Alzheimer's disease. *Nat Genet* 43(5):436-+.

3. Jun G (2011) Meta-analysis Confirms CR1, CLU, and PICALM as Alzheimer Disease Risk Loci and Reveals Interactions With APOE Genotypes (vol 67, pg 1473, 2010). *Arch Neurol-Chicago* 68(2):159-159.

4. Lee JH, Cheng R, Graff-Radford N, Foroud T, & Mayeux R (2008) Analyses of the national institute on aging late-onset alzheimer's disease family study: implication of additional loci. *Arch Neurol-Chicago* 65(11):1518-1526.

5. Purcell S, *et al.* (2007) PLINK: A tool set for whole-genome association and population-based linkage analyses. *Am J Hum Genet* 81(3):559-575.

6. Das S, *et al.* (2016) Next-generation genotype imputation service and methods. *Nat Genet* 48(10):1284-1287.

7. McCarthy S, *et al.* (2016) A reference panel of 64,976 haplotypes for genotype imputation. *Nat Genet* 48(10):1279-1283.

8. Loh PR, *et al.* (2016) Reference-based phasing using the Haplotype Reference Consortium panel. *Nat Genet* 48(11):1443-1448.

9. Jun G, Wing MK, Abecasis GR, & Kang HM (2015) An efficient and scalable analysis framework for variant extraction and refinement from population-scale DNA sequence data. *Genome Res* 25(6):918-925.

10. Andrews S (FastQC A Quality Control tool for High Throughput Sequence Data. http://www.bioinformatics.babraham.ac.uk/projects/fastqc/.

11. Bolger AM, Lohse M, & Usadel B (2014) Trimmomatic: a flexible trimmer for Illumina sequence data. *Bioinformatics* 30(15):2114-2120.

12. Browning SR & Browning BL (2007) Rapid and accurate haplotype phasing and missing-data inference for whole-genome association studies by use of localized haplotype clustering. *Am J Hum Genet* 81(5):1084-1097.

13. Browning BL & Browning SR (2009) A Unified Approach to Genotype Imputation and Haplotype-Phase Inference for Large Data Sets of Trios and Unrelated Individuals. *Am J Hum Genet* 84(2):210-223.

14. Danecek P, *et al.* (2011) The variant call format and VCFtools. *Bioinformatics* 27(15):2156-2158.

15. Abraham G & Inouye M (2014) Fast Principal Component Analysis of Large-Scale Genome-Wide Data. *PLoS One* 9(4).

16. Price AL, *et al.* (2006) Principal components analysis corrects for stratification in genome-wide association studies. *Nat Genet* 38(8):904-909.

17. Raj A, Stephens M, & Pritchard JK (2014) fastSTRUCTURE: Variational Inference of Population Structure in Large SNP Data Sets. *Genetics* 197(2):573-U207.

18. Consortium GT (2015) Human genomics. The Genotype-Tissue Expression (GTEx) pilot analysis: multitissue gene regulation in humans. *Science* 348(6235):648-660.

19. Consortium GT (2013) The Genotype-Tissue Expression (GTEx) project. *Nature genetics* 45(6):580-585.

20. Karssen L & Team G (2013) New Software and Developments in the GenABEL Project. *Hum Hered* 76(2):111-111.

21. Cai N, *et al.* (2017) 11,670 whole-genome sequences representative of the Han Chinese population from the CONVERGE project. *Sci Data* 4:170011.

22. Mueller SG, *et al.* (2005) Ways toward an early diagnosis in Alzheimer's disease: the Alzheimer's Disease Neuroimaging Initiative (ADNI). *Alzheimers Dement* 1(1):55-66.

23. Lambert JC, *et al.* (2013) Meta-analysis of 74,046 individuals identifies 11 new susceptibility loci for Alzheimer's disease. *Nat Genet* 45(12):1452-1458.

ADNI I, GO, II and III studies

Andrew J. Saykin, Arthur W. Toga, Bret Borowski, Chad Ward, Charles DeCArli, Chet Mathis, Clifford R. Jack, Jr., Danielle Harvey, David Holtzman, David Jones, Devon Gessert, Eli Lilly, Eric M. Reiman, Erin Franklin, Franz Hefti, Greg Sorensen, Gustavo Jimenez, Howard Fillit, Jeff Gunter, Jennifer Salazar, John Hsiao, John Morris, John Q. Trojanowki, Karen Crawford, Scott Neu, Kejal Kantarci, Kelley Faber, Kelly Harless, Kewei Chen, Kwangsik Nho, Laurel, Beckett, Lean Thal, Leon Thal, Leslie M. Shaw , Lew Kuller, Li Shen, Lindsey Hergesheimer, Lisa Taylor-Reinwald, M. Marcel Mesulam, Magdalena Korecka, Marc Raichle, Maria, Carrillo, Marilyn Albert, Matt Senjem, Matthew Bernstein, Michael Donohue, Michael Weiner, Michal Figurski, Neil Buckholtz, Nick Fox, Nigel J. Cairns, Norbert Schuff, Norm Foster, Paul Aisen, Paul Thompson, Peter Davies, Peter J. Snyder, Peter Snyder, Prashanthi Vemuri, Richard Frank, Robert A. Koeppe, Robert C. Green, Ronald Petersen, Sarah Walter, Steven Paul, Steven Potkin, Sungeun Kim, Tatiana M. Foroud, Tom Montine, Virginia Lee, William Jagust, William Potter, Yuliana Cabrera, Zaven Khachaturian

Investigators of ADNI from university and institutes

Adam Fleisher, Aimee Pierce, Akiva Mintz, Alan Lerner, Alexander Norbash, Allan I. Levey, Allyson Rosen, Amanda Smith, Anaztasia Ulysse, Andrew E. Budson, Andrew Kertesz, Angela Oliver, Ann Marie Hake, Anna Burke, Antero Sarrael, Anton P. Porsteinsson, Ashley Lamb, Athena Lee, Balebail Ashok Raj, Barton Lane, Beatriz Yanez, Beau Ances, Benita Mudge, Betty Lind, Bojana Stefanovic, Bonnie S. Goldstein, Borna Bonakdarpour, Brandy R. Matthews, Brian R. Ott, Brigid Reynolds, Bruce L. Miller, Bryan M. Spann, Carl Sadowsky, Charles Bernick, Charles D. Smith, Chiadi Onyike, Chris (Chinthaka) Heyn, Chris Hosein, Christi Leach, Christine M. Belden, Christopher H. van Dyck, Christopher M. Clark, Chuang-Kuo Wu, Colleen S. Albers, Connie Brand, Courtney Bodge, Curtis Tatsuoka, Cynthia M. Carlsson, Dana Mathews, Daniel D'Agostino II, Daniel H.S. Silverman, Daniel Marson, David A. Wolk, David Bachman, David Clark, David Geldmacher, David Hart, David Knopman, David Perry, David Winkfield, Delwyn D. Miller, Diana Kerwin, Dick Drost, Donna M. Simpson, Donna Munic, Douglas W. Scharre, Dr Rob Bartha, Dzintra Celmins, Earl A. Zimmerman, Edmond Teng, Edward Coleman, Edward Zamrini, Effie Mitsis, Elizabeth Finger, Elizabeth Oates, Elizabeth Sosa, Ellen Woo, Emily Rogalski, Evan Fletcher, Francine Parfitt, Gaby Thai, Gad A. Marshall, Gary Conrad, Geoffrey Tremont, George Bartzokis, Ging-Yuek Robin Hsiung, Gloria Chiang, Godfrey D. Pearlson, Greg Jicha, Helen Vanderswag, Hillel Grossman, Horacio Capote, Howard Bergman, Howard Chertkow, Howard Feldman, Howard J. Rosen, Hristina Koleva, Hyungsub Shim, Irina Rachinsky, Jacobo Mintzer, Jaimie Ziolkowski, James Brewer, James J. Lah, Jamika, Singleton-Garvin, Janet S. Cellar, Jared R. Brosch, Jared Tinklenberg, Jason H. Karlawish, Javier Villanueva-Meyer, Jeffrey A. Kaye, Jeffrey M. Burns, Jeffrey R. Petrella, Jerome Yesavage, Joanne Allard, Joanne L. Lord, Joel Hetelle, John Brockington, John C. Morris, John Olichney, John Rogers, Joseph Quinn, Joseph S. Kass, Joy L. Taylor, Judith L. Heidebrink, Karen Anderson, Karen Blank, Karen Ekstam Smith, Karen L. Bell, Kathleen Johnson, Kathleen Tingus, Kathryn DeMarco, Kaycee M. Sink, Keith A. Johnson, Kelly M. Makino, Kenneth Spicer, Ki Won Nam, Kim Martin, Kim Poki-Walker, Kris Johnson, Kristin Fargher, Kristine Lipowski, Kyle Womack, Laura A. Flashman, Lawrence S. Honig, Liana Apostolova, Liberty Teodoro, Lisa C. Silbert, Lisa Ravdin, Lon S. Schneider, Lori A. Daiello, M. Saleem Ismail, Marc Seltzer, Marek-Marsel Mesulam, Maria

Carroll, Maria Kataki, Maria T. GreigCusto, Marissa Natelson Love, Mark A. Mintun, Martin R. Farlow, Martin Sadowski, Mary L. Creech, Mary L. Hynes, Mary Quiceno, MaryAnn Oakley, Mauricio Becerra, Megan Witbracht, Melanie Keltz, Melissa Lamar, Mia Yang, Michael Borrie, Michael Lin, Michele Assaly, Michelle Rainka, Mimi Dang, Mohammed O. Sheikh, Mrunalini Gaikwad, Munir Chowdhury, Nadira Trncic, Nancy Johnson, Nancy Kowalksi, Nathaniel Pacini, Neil Kowall, Neill R Graff-Radford, Norman Relkin, Ntekim E. Oyonumo, Nunzio Pomara, Olga James, Olu Ogunlana, Oscar L. Lopez, Owen Carmichael, P. Murali Doraiswamy, Parianne Fatica, Patricia Lynn Johnson, Patricia Samuels, Paul Malloy, Paula Ogrocki, Pauline Maillard, Peter Hardy, Pierre Tariot, Po H. Lu, Pradeep Varma, Rachelle S. Doody, Raina Carter, Raj C. Shah, Randall Griffith, Randy Yeh, Ranjan Duara, Rawan Tarawneh, Raymond Scott Turner, Raymundo Hernando, Reisa A., Richard E. Carson, Riham El Khouli, Robert B. Santulli, Ronald Killiany, Rosemarie Rodriguez, Russell H. Swerdlow, Salvador Borges-Neto, Sandra Black, Sandra Weintraub, Sanjay Asthana, Sanjeev Vaishnavi, Sara Dolen, Sara S. Mason, Scott Herring, Sherye A. Sirrel, Smita Kittur, Sonia Pawluczyk, Stacy Schneider, Stephanie Kielb, Stephanie Reeder, Stephen Correia, Stephen Pasternack, Stephen Pasternak, Stephen Salloway, Sterling Johnson, Steven Chao, Steven E. Arnold, Susan K. Schultz, Susan Rountree, T-Y Lee, Terence Z. Wong, Teresa Villena, Thomas O. Obisesan, Valory Pavlik, Vernice Bates, Vesna Sossi, Victoria Shibley, William M. Brooks, William Pavlosky, Yaakov Stern

Biomarkers Consortium Project Team Members

Adam Simon, Ashok Dongre, Bob Dean, Brad Navia, Dan Spellman, David Lee, David Shera, Eric Siemers, Eve Pickering, Frank Swenson, Fred Immerman, George Nomikos, Holly Soares, Hong Wan, Jeff Seeburger, Jeff Waring, John Trojanowski, Judy Siuciak, Kevin Duffin, Les Shaw, Li-San Wang, Madhav Thambisetty, Marc Walton, Mary Savage, Mats Ferm, Max Kuhn, Neil Buckholtz, Panos Zagouras, Patricia Cole, Ron Hendrickson, Sharon Xie, Sophie Allauzen, Walter Koroshetz, William Potter